THE JOURNAL OF PHYSICAL CHEMISTRY Letters

Letter

pubs.acs.org/JPCL

Product Branching in the Low Temperature Reaction of CN with Propyne by Chirped-Pulse Microwave Spectroscopy in a Uniform Supersonic Flow

Chamara Abeysekera,[†] Baptiste Joalland,[†] Nuwandi Ariyasingha,[†] Lindsay N. Zack,[†] Ian R. Sims,[‡] Robert W. Field,[§] and Arthur G. Suits*[,†]

[†]Department of Chemistry, Wayne State University, 5101 Cass Avenue, Detroit, Michigan 48202, United States

[‡]Institut de Physique de Rennes, UMR CNRS-UR1 6251, Université de Rennes 1, 263 Avenue du Général Leclerc, 35042, Rennes CEDEX, France

[§]Department of Chemistry, Massachusetts Institute of Technology, Cambridge, Massachusetts 02139, United States

Supporting Information

ABSTRACT: A new chirped-pulse/uniform flow (CPUF) spectrometer has been developed and used to determine product branching in a multichannel reaction. With this technique, bimolecular reactions can be initiated in a cold, thermalized, high-density molecular flow and a broadband microwave spectrum acquired for all products with rotational transitions within a chosen frequency window. In this work, the CN + CH_3CCH reaction was found to yield HCN via a direct H-abstraction reaction, whereas indirect addition/elimination pathways to HCCCN, CH_3CCCN, and CH_2CCHCN were also probed. From these observations, quantitative branching ratios were established for all products as 12(5)%, 66(4)%, 22(6)%, and 0(8)% into HCN, HCCCN, CH_3CCCN, and CH_2CCHCN, respectively. The values are consistent with statistical calculations based on new ab initio results at the CBS-QB3 level of theory. This work is a demonstration of CPUF as a powerful technique for quantitatively determining the branching into polyatomic products from a bimolecular reaction.

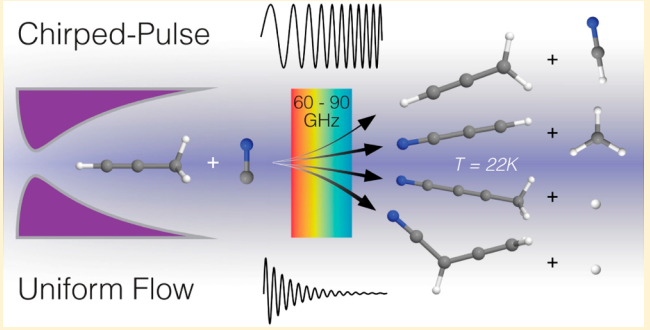

The interplay between fundamental laboratory investigations, theoretical advances, and chemical modeling has led to tremendous progress over the past decade in understanding complex gas-phase environments, from cold interstellar clouds to combustion systems.[1,2] Measured or calculated reaction rates for thousands of elementary reactions are incorporated into models of chemistry under extreme conditions to identify key pathways that control reaction outcomes. However, nearly all kinetics studies report the observed rate of *reactant disappearance*, with product identity and branching largely unknown. This limitation arises from considerable experimental challenges inherent in the quantitative detection of the full range of products of a given reaction, particularly for large polyatomic systems. Recent advances have relied upon tunable synchrotron photoionization or low-energy electron impact ionization to achieve selective product detection in dynamics, kinetics, and flame studies.[3−6] These pioneering studies have demonstrated a general capability for isomer-specific product branching determination in flame studies, kinetics, and crossed-beam scattering, highlighting the importance of such information for accurate kinetic modeling. Challenges remain, however, as these studies require fitting of composite and often incompletely resolved spectra to infer branching, and clear product signatures are often lacking.

We have developed an alternative approach to address this challenge, which incorporates chirped-pulse microwave spectroscopy in low-temperature uniform supersonic flows ("chirped-pulse/uniform flow", CPUF).[7,8] This technique, relying on chirped-pulse Fourier-transform microwave spectroscopy,[9−15] provides clear quantifiable spectroscopic signatures of polyatomic products in bimolecular or unimolecular reactions for virtually any species with a modest electric dipole moment.

One class of reactions well-suited to this new technique involves the cyano radical owing to the large dipole moments of the products and given its importance in combustion and astrochemistry. In combustion, both the CN radical and HCN have been detected as intermediates or products from the burning of hydrocarbons in the presence of nitrogen. These species can then play a key role in NO_x formation/destruction mechanisms and in nitrile incorporation in soot formation

Received: March 11, 2015
Accepted: April 10, 2015
Published: April 10, 2015

DOI: 10.1021/acs.jpclett.5b00519
J. Phys. Chem. Lett. 2015, 6, 1599−1604

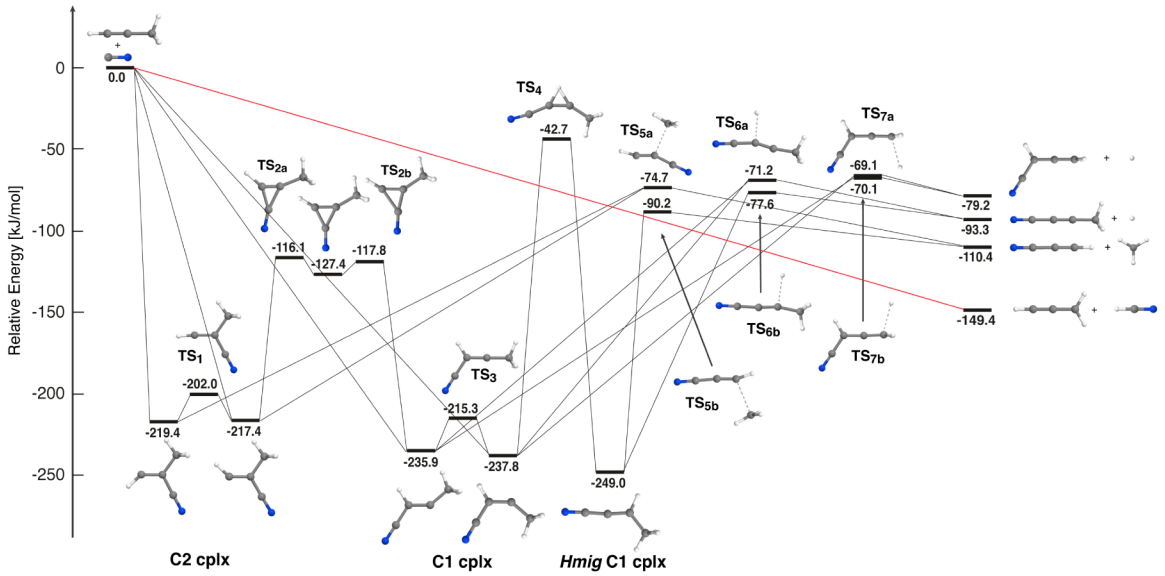

Figure 1. Key stationary points on the potential energy surface for the CN + CH_3CCH reaction, calculated at CBS-QB3 level of theory.

processes. In the interstellar medium (ISM), more than 30 species that contain a CN group have been detected, from small metal cyanides in circumstellar envelopes to large (>6 atoms) organic species in dense molecular clouds.[16−21] Within the solar system, Saturn's moon Titan is enveloped by a yellowish haze that is attributed to nitrile- and hydrocarbon-rich aerosol haze layers.[22−25] However, despite the ubiquity of this class of molecules in the ISM and in combustion systems, the formation mechanisms are still poorly understood. Nonetheless, some insight has been gained from gas-phase kinetic measurements for reactions between the CN radical and several hydrocarbons at temperatures down to 13 K.[26−31] Other investigations have been carried out using crossed-molecular beam methods to characterize the reaction dynamics and identify the reaction products for this class of reaction.[32,33] Despite this effort, the determination of detailed product branching remains challenging.

Here, a detailed study of the reaction of the cyano radical with propyne using the CPUF technique is presented. Line intensities from rotational spectra have been used to determine the product branching from each of the accessible reaction pathways:

Direct abstraction

$$CN + CH_3CCH \rightarrow HCN + CH_2CCH \quad (I)$$

CN addition/methyl elimination

$$CN + CH_3CCH \rightarrow CH_3 + HCCCN \quad (II)$$

CN addition/H elimination

$$CN + CH_3CCH \rightarrow H + CH_3CCCN \quad (III)$$

$$CN + CH_3CCH \rightarrow H + CH_2CCHCN \quad (IV)$$

With support of ab initio and statistical calculations, these measurements reveal the underlying dynamics of this reaction, thus providing important insights for the modeling of complex gas-phase environments.

To guide the spectroscopic investigation, the ground−state potential energy CN + propyne surface (Figure 1) was modeled at the CBS-QB3 level of theory. First, there is a direct barrierless abstraction path to form HCN and propargyl radical that is exoergic by 149 kJ mol^{-1}. We also find two barrierless C1 *cis*/*trans* addition complexes, bound by over 230 kJ mol^{-1} and separated by a 22.5 kJ mol^{-1} isomerization barrier, largely consistent with the previous theoretical work.[34,35] In addition, a barrierless C2 addition complex, 18.5 kJ mol^{-1} higher in energy than the *trans*-C1 complex, is also present. There is an isomerization barrier of ∼100 kJ mol^{-1} separating the C1 and C2 complexes, which is considerably lower than any exit pathway; thus, equilibration between these complexes prior to dissociation is very likely at these low collision energies. The lowest energy exit pathway from the addition complexes leads over TS5b to methyl elimination and cyanoacetylene formation. The C1 complexes can pass over TS6b, slightly higher than TS5b, to yield H + cyanomethylacetylene; at a yet slightly higher energy, they may pass over TS7b to give H + cyanoallene. Another possibility for the C1 complexes is to pass over a 195 kJ mol^{-1} H migration barrier TS4 to form the HmigC1 complex. This H migrated complex has the lowest exit barrier, 158.8 kJ mol^{-1} and it yields the methyl elimination product. Thus, the potential energy surface suggests that the reaction products listed in eqs I−IV are appropriate targets for a spectroscopic investigation. Rice−Ramsperger−Kassel−Marcus (RRKM) calculations of energy-dependent rate constants for all individual unimolecular steps were also performed as described further in the Supporting Information.

The CPUF apparatus (Figure 2) has two main components: a chirped pulse broadband microwave spectrometer and a pulsed uniform flow system built around a high-throughput pulsed Laval nozzle.[8,36] A broadband frequency chirp (in the 60—90 GHz region) is broadcast into the pulsed uniform flow at a series of intervals after a laser fires to initiate the reaction. All molecules with a dipole moment and with rotational transitions in the scanned frequency range are polarized by the radiation. The free induction decay (FID) of the polarized sample is collected through the detection feed horn, amplified, and sent to a digital oscilloscope for time-domain averaging and signal processing. The Fourier transform of the FID gives the full broadband frequency domain spectrum.

The ∼22 K flow[8] consists of 0.5% BrCN and 1.5% propyne in helium, and the reaction is initiated by 193 nm photodissociation of BrCN. Successive spectra were obtained at 10 μs

DOI: 10.1021/acs.jpclett.5b00519
J. Phys. Chem. Lett. 2015, 6, 1599−1604

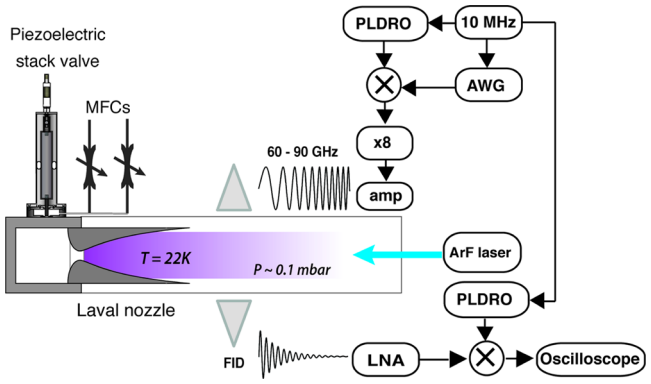

Figure 2. Schematic for CPUF. Linearly chirped pulses (0.25−3.75 GHz) are produced in an arbitrary waveform generator (AWG) and then mixed with a PLDRO (frequency 8.125 GHz) locked to a 10 MHz Rb standard. The resulting frequencies are then multiplied, amplified, and broadcast onto the flow via a feedhorn that is oriented perpendicular to the flow axis. Bandpass filters and isolators are inserted into the setup as necessary. The pulsed uniform flow source consists of a piezoelectric stack valve,[36] connected to mass flow controllers (MFC), and a Laval nozzle mounted on one end of a polycarbonate vacuum chamber.[8] A quartz window is located on the other end of the chamber to allow radiation from an ArF excimer laser to propagate down the axis of the Laval nozzle, such that the core of the flow is irradiated. The resultant molecular emission from the core is collected as free induction decay (FID) by a second feedhorn, amplified through a low noise amplifier (LNA), downconverted before detection, and phase-coherently averaged in an oscilloscope, where it is fast Fourier transformed to produce a frequency-domain spectrum.

intervals following the laser trigger and the first chirped pulse excitation.[37] Twelve frames (i.e. 12 independent spectra) were obtained in this fashion for each gas pulse, with each frame averaged for roughly 62500 acquisitions. All bimolecular reaction products began to appear approximately 50 μs after the laser trigger and show a slow rise followed by a more abrupt rise at 80−90 μs (see Supporting Information), which is consistent with our previous observations.[7] The delay in the initial appearance is likely owing to rotational cooling of the CN prior to reaction, as it is known to be formed vibrationally cold but rotationally hot from 193 nm photolysis of BrCN.[38,39] Rotational and vibrational thermalization of the products may also contribute to this delay. The average of the eighth and ninth frames were used to determine the branching reported here. We note that the rise at later times may include some contribution from reaction occurring in the nozzle throat that may not have reached the 22 K flow temperature, but this is not likely to impact the measured branching. The disappearance of the products at longer times is owing to the passage of the reacting sample out of the probe region. We emphasize that we are not measuring reaction rate coefficients, only product branching. Our analysis assumes product thermalization.

Figure 3 shows spectra recorded over two frequency regions. The top spectrum (Figure 3a) was collected using segmented macrochirps (50 MHz bandwidth each) over a total 1.5 GHz range. In this fashion, the strongest transitions of the indirect-channel products could be probed: HCCCN (J = 9−8 transition at 81.881 GHz), CH_3CCCN (J_K = 20_0−19_0 at 82.627 GHz) and CH_2CCHCN ($J_{Ka,Kc}$ = $16_{0,16}$−$15_{0,15}$ at 81.674 GHz). HCCCN and CH_3CCCN were clearly detected; however, CH_2CCHCN was not. Additional spectral lines are present, most of which are attributable to the BrCN precursor.

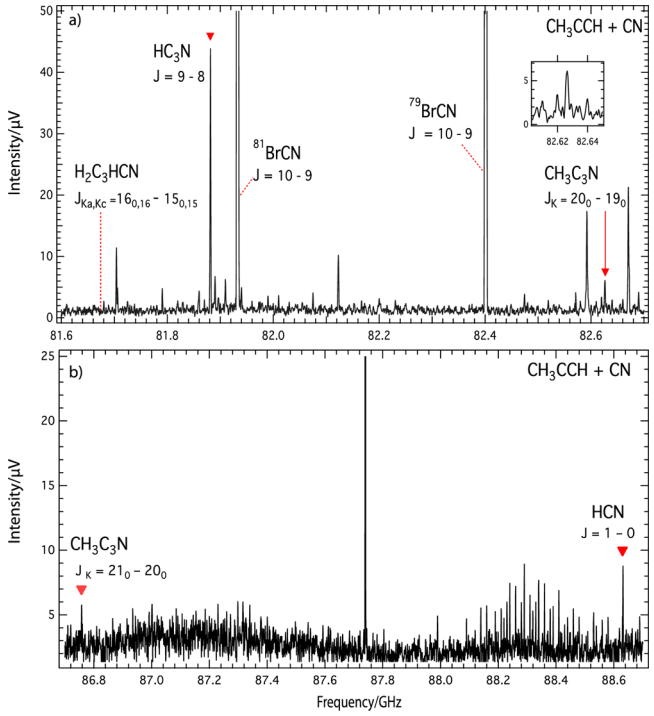

Figure 3. Chirped-pulse Fourier transform microwave spectra for reaction products of the CN + propyne reaction. (A) Segmented macrochirp scan that targets transitions of HCCCN, CH_2CCHCN, and CH_3CCCN; J = 9−8 transition at 81.881 GHz, $J_{Ka,Kc}$ = $16_{0,16}$−$15_{0,15}$ at 81.674 GHz and J_K = 20_0−19_0 at 82.627 GHz. The inset shows the K = 0, 1, 2, and 3 transitions of CH_3CCCN. (B) Broad scan from 86.63 to 88.73 GHz that targets the $J_{Ka,Kc}$ = $17_{0,17}$−$16_{0,16}$ transition of CH_2CCHCN at 86.668 GHz, the J_K = 21_0−20_0 transition of CH_3CCCN at 86.750 GHz, and the J = 1−0 transition of HCN at 88.631 GHz. Each spectrum is averaged for 125 000 laser shots.

Time sequence spectra and integrated kinetic traces are given in Supporting Information.

Figure 3b shows a broad 86.63−88.73 GHz scan, covering the $J_{Ka,Kc}$ = $17_{0,17}$−$16_{0,16}$ transition of CH_2CCHCN at 86.668 GHz, the J_K = 21_0−20_0 transition of CH_3CCCN at 86.750 GHz, and the J = 1−0 transition of HCN at 88.631 GHz. Again, CH_2CCHCN was not observed, although both CH_3CCCN and the direct product HCN were observed, which allows comparison between the direct and indirect reaction pathways.

We have considered the possibility that primary products of the CN + CH_3CCH reaction go on to react further. However, as detailed in the Supporting Information, all possible secondary reactions are too slow to contribute on the time scale of the experiment, so this interference is deemed unlikely. Control experiments were also performed and all signals were found to require the two reactants and the photolysis laser. We also performed a scan over the HCN region with allene substituted for propyne. No HCN was seen. Given the fact that propyne and allene show the same photochemistry at 193 nm[40] but allene has a 4-fold larger absorption cross section, this result strongly suggests that propyne photochemistry does not contribute to the observed HCN signals.

Relative product populations (branching) can be calculated using the relationship between the integrated line intensities (W) and column densities (N_{tot})

DOI: 10.1021/acs.jpclett.5b00519
J. Phys. Chem. Lett. 2015, 6, 1599−1604

$$W = \frac{4\pi^{3/2}\omega_0^2 S\mu_i^2 g_I g_K \varepsilon}{c\sqrt{\alpha}} \frac{N_{tot}}{kT_{rot}Q_{rot}} e^{-E_l/kT_{rot}} \quad (1)$$

with k the Boltzmann constant, ω_0 the transition frequency, α the sweep rate, and Q_{rot} and T_{rot} the partition function and rotational temperature, respectively. The quantities S, μ_i, g_I, and g_K represent the line strength, dipole moment, nuclear spin weight, and K degeneracy.[41] Fractional abundances relative to CH_3CCCN were calculated for each product using their respective integrated line intensities. For CH_2CCHCN, an *upper limit* to its abundance could be obtained from the noise level of the spectrum. Although the spectra shown in Figure 3 were collected separately, the presence of CH_3CCCN in both spectra enabled scaling of the two scans. Thus, quantitative branching ratios could be determined between the direct (HCN) and indirect (HCCCN, CH_3CCCN) reaction pathways. Error bars (2σ) on the branching were based on the uncertainty in the spectral line widths and intensities for each species, determined from Gaussian fits of each line. No other sources of error were assumed.

Experimental and calculated branching ratios for this reaction are shown in Table 1. The CPUF results include the HCCCN and CH_3CCCN products arising from indirect addition/elimination reactions and the HCN product from direct H abstraction. The RRKM results are only applicable to branching between the various addition−elimination channels (i.e. indirect pathways); thus, they have been adjusted accordingly to account for the measured branching into the direct channel.

Experimental results show the branching between the direct and indirect channels to be roughly 12% to 88%, respectively. The fairly small branching to the direct reaction is perhaps not surprising despite the exoergicity given the low collision energy and the strong electrophilic interaction of CN with the propyne π system. The indirect addition/elimination pathway produces three possible products: HCCCN by CH_3 elimination and CH_3CCCN and CH_2CCHCN from H elimination, with experimentally determined branching of 66%, 22%, and an upper bound of 8%, respectively. RRKM calculations initiated at the C1 and C2 minima support this result, with 48 or 65% into HCCCN and 33 or 19% into CH_3CCCN, respectively. These values are also consistent with the fact that that HCCCN is the lowest-energy product in this pathway and can be produced from either the HmigC1 or C2 complex. Both CH_3CCCN and CH_2CCHCN can also arise from either C1 adducts, but not from C2. From either C1 complex, the pathway leading to CH_3CCCN formation has a lower exit barrier, making it the more favorable of the H elimination products.

Table 1. Product Branching, in Percent, for the Reaction of CN with CH_3CCH at 22 K with 2σ Uncertainty in the Last Digit[a]

		addition−elimination			direct abstraction
		HCCCN	CH_3CCCN	CH_2CCHCN	HCN
CPUF		66(4)	22(6)	0(8)	12(5)
RRKM	C1 cplx	48	33	7	
	C2 cplx	65	19	4	

[a]RRKM calculations for the product branching in the addition/elimination reactions starting from either C1 or C2 addition complexes.

These results can also be compared to previous crossed molecular beam (CMB) studies conducted at collision energy of 27 kJ mol^{-1}.[34,35,42] The CMB studies only reported detection of the H elimination products, and based upon selective deuterium labeling, nearly equal branching to the two H loss products was inferred. This estimate required some assumptions about product detection efficiencies and also neglects the isotope dependence of the decomposition, which may well be important for H elimination. In general, these CMB investigations suffer from kinematic constraints that favor detection of products with small center-of-mass recoil velocities. As such, the CMB studies were unable to detect the CH_3 elimination product, HCCCN, or the direct reaction to HCN.

The good agreement between the theoretical and observed product branching underscores the ability of CPUF to obtain reliable branching among competing channels and their products. CPUF can provide detailed product branching with unambiguous, isomer-specific product detection, adding a powerful new tool to the reaction dynamics repertoire for polyatomic systems that includes CMB methods with electron impact detection as well as synchrotron-based VUV photoionization.

EXPERIMENTAL SECTION

The spectrometer consists of an 8 gigasamples/s arbitrary waveform generator (AWG; Tektronix AWG7082C), which is used to produce a linear frequency sweep, and a phase-locked dielectric resonator oscillator (PLDRO) at 8.125 GHz to upconvert the AWG pulse via a broadband mixer (Marki M10418LC). The mixer output is amplified with a broadband amplifier (ALC Microwave ALS030283), and the desired band is selected through a bandpass filter and propagated through a 8× multiplication stage to obtain the final frequency of 60−90 GHz with an output power of ∼100 mW. Typical chirp duration was ∼1 μs with FID collection for 1−2 μs. The laser and gas pulse were operated at 3.5 Hz.

The final frequencies were transmitted via a feedhorn into the high-density polycarbonate uniform flow chamber where the bimolecular reaction is initiated. The free induction decay (FID) of the polarized sample is collected through the detection feed horn, amplified with a low noise amplifier (LNA; Miteq AMF-4D-00100800-18-13P), downconverted, and sent to a digital oscilloscope (Tektronix DPO70804C) for time-domain averaging and signal processing.

In order to achieve a uniform mixture throughout the scans, two mass flow controllers (Bronkhorst EL-Flow) were used. Pure He gas (600 sccm) was passed over solid cyanogen bromide (BrCN; Sigma-Aldrich, 97%) at room temperature with a backing pressure of 3 bar. The output was mixed with a 9 sccm flow of pure methylacetylene (Sigma-Aldrich, 99%) to obtain a 1.5% mixture of CH_3CCH in BrCN/He. Total density in the flow was ∼3.8 × 10^{16} cm^{-3}. An excimer laser (GAM Laser, EX200/60) with 60 mJ/pulse of 193 nm (loosely focused to a fluence of ∼100 mJ/cm^2) was used to photodissociate BrCN and produce the CN radical at an estimated density of 5 × 10^{13} cm^3. Additional details are provided in our previous publication.[7]

Computational. Electronic structure calculations were performed at the CBS-QB3 level of theory, which extrapolate the energetics at the complete basis limit in order to obtain an accuracy of ∼5 kJ mol^{-1} after zero-point energy correction. This composite method involves geometry optimization and

DOI: 10.1021/acs.jpclett.5b00519
J. Phys. Chem. Lett. 2015, 6, 1599−1604

vibrational frequency calculation at the B3LYP/6-311G(2d,d,p) level; the same vibrational frequencies were used to compute the partition functions of the different minima and saddle points in the Rice−Ramsperger−Kassel−Marcus (RRKM) calculations of energy-dependent rate constants for all individual unimolecular steps. These rate constants were estimated at an internal energy fixed by the reactant asymptote, and we assumed that the available energy was converted to internal vibrational energy.

■ ASSOCIATED CONTENT

Supporting Information

Energies, structures, and vibrational frequencies of the different minima and transition states of the complex-mediated pathways in the CN + C_3H_4 potential energy surface, along with the RRKM unimolecular reaction rates used to determine the branching ratios presented in the paper. All optimizations were performed at the CBS-QB3 level of theory with the Gaussian 09 package. The reaction rates take into account semiclassical tunneling correction using the Eckart method. In addition, we include plots of the raw time sequences and the integrated kinetic traces for the spectra. This material is available free of charge via the Internet at http://pubs.acs.org.

■ AUTHOR INFORMATION

Corresponding Author

*E-mail: asuits@wayne.edu.

Notes

The authors declare no competing financial interest.

■ ACKNOWLEDGMENTS

The National Science Foundation (NSF), Award MRI-ID 1126380 and Department of Energy (DOE)/Basic Energy Sciences (BES) award DE FG02-04ER15593 supported this work. We thank Kirill Prozument for assistance with the spectrometer and Alex Mebel for providing the RRKM code.

■ REFERENCES

(1) Tielens, A. The Molecular Universe. *Rev. Mod. Phys.* **2013**, *85*, 1021.

(2) Wakelam, V.; Smith, I. W. M.; Herbst, E.; Troe, J.; Geppert, W.; Linnartz, H.; Öberg, K.; Roueff, E.; Agúndez, M.; Pernot, P. Reaction Networks for Interstellar Chemical Modelling: Improvements and Challenges. *Space Sci. Rev.* **2010**, *156*, 13−72.

(3) Suits, A. G. Photodissociation and Reaction Dynamics Studies Using Third-Generation Synchrotron Radiation. *Chemical Applications of Synchrotron Radiation. Part I: Dynamics and VUV Spectroscopy. Part II: X-Ray Applications*; Sham, T.-K., Ed.; World Scientific Publishing Company: Singapore, 2002; Vol. *12*, pp 3−54.

(4) Trevitt, A. J.; Soorkia, S.; Savee, J. D.; Selby, T. S.; Osborn, D. L.; Taatjes, C. A.; Leone, S. R. Branching Fractions of the CN+ C3H6 Reaction Using Synchrotron Photoionization Mass Spectrometry: Evidence for the 3-Cyanopropene Product. *J. Phys. Chem. A* **2011**, *115*, 13467−13473.

(5) Hansen, N.; Miller, J. A.; Westmoreland, P. R.; Kasper, T.; Kohse-Höinghaus, K.; Wang, J.; Cool, T. A. Isomer-Specific Combustion Chemistry in Allene and Propyne Flames. *Combust. Flame* **2009**, *156*, 2153−2164.

(6) Casavecchia, P.; Leonori, F.; Balucani, N.; Petrucci, R.; Capozza, G.; Segoloni, E. Probing the Dynamics of Polyatomic Multichannel Elementary Reactions by Crossed Molecular Beam Experiments with Soft Electron-Ionization Mass Spectrometric Detection. *Phys. Chem. Chem. Phys.* **2009**, *11*, 46−65.

(7) Abeysekera, C.; Zack, L. N.; Park, G. B.; Joalland, B.; Oldham, J. M.; Prozument, K.; Ariyasingha, N. M.; Sims, I. R.; Field, R. W.; Suits, A. G. A Chirped-Pulse Fourier-Transform Microwave/Pulsed Uniform Flow Spectrometer. II. Performance and Applications for Reaction Dynamics. *J. Chem. Phys.* **2014**, *141*, 214203.

(8) Oldham, J. M.; Abeysekera, C.; Joalland, B.; Zack, L. N.; Prozument, K.; Sims, I. R.; Park, G. B.; Field, R. W.; Suits, A. G. A Chirped-Pulse Fourier-Transform Microwave/Pulsed Uniform Flow Spectrometer. I. The Low-Temperature Flow System. *J. Chem. Phys.* **2014**, *141*, 154202.

(9) Brown, G. G.; Dian, B. C.; Douglass, K. O.; Geyer, S. M.; Shipman, S. T.; Pate, B. H. A Broadband Fourier Transform Microwave Spectrometer Based on Chirped Pulse Excitation. *Rev. Sci. Instrum.* **2008**, *79*, 053103.

(10) Dian, B. C.; Brown, G. G.; Douglass, K. O.; Pate, B. H. Measuring Picosecond Isomerization Kinetics via Broadband Microwave Spectroscopy. *Science* **2008**, *320*, 924−928.

(11) Park, G. B.; Steeves, A. H.; Kuyanov-Prozument, K.; Neill, J. L.; Field, R. W. Design and Evaluation of a Pulsed-Jet Chirped-Pulse Millimeter-Wave Spectrometer for the 70−102 GHz Region. *J. Chem. Phys.* **2011**, *135*, 024202.

(12) Endo, Y.; Tsuchiya, S.; Yamada, C.; Hirota, E.; Koda, S. Microwave Kinetic Spectroscopy of Reaction Intermediates: O +Ethylene Reaction at Low Pressure. *J. Chem. Phys.* **1986**, *85*, 4446.

(13) Koda, S.; Endo, Y.; Hirota, E. Branching Ratios in O(3P) Reactions of Terminal Olefins Studied by Kinetic Microwave Absorption Spectroscopy. *J. Phys. Chem.* **1991**, *95*, 1241−1244.

(14) Prozument, K.; Barratt Park, G.; Shaver, R. G.; Vasiliou, A. K.; Oldham, J. M.; David, D. E.; Muenter, J. S.; Stanton, J. F.; Suits, A. G.; Barney Ellison, G.; et al. Chirped-Pulse Millimeter-Wave Spectroscopy for Dynamics and Kinetics Studies of Pyrolysis Reactions. *Phys. Chem. Chem. Phys.* **2014**, *16*, 15739−15751.

(15) Kidwell, N. M.; Vaquero-Vara, V.; Ormond, T. K.; Buckingham, G. T.; Zhang, D.; Mehta-Hurt, D. N.; McCaslin, L.; Nimlos, M. R.; Daily, J. W.; Dian, B. C.; et al. Chirped-Pulse Fourier Transform Microwave Spectroscopy Coupled with a Flash Pyrolysis Microreactor: Structural Determination of the Reactive Intermediate Cyclopentadienone. *J. Phys. Chem. Lett.* **2014**, *5*, 2201−2207.

(16) Jamal, A.; Mebel, A. M. Theoretical Investigation of the Mechanism and Product Branching Ratios of the Reactions of Cyano Radical with 1-and 2-Butyne and 1,2-Butadiene. *J. Phys. Chem. A* **2013**, *117*, 741−755.

(17) Broten, N. W.; Oka, T.; Avery, L. W.; MacLeod, J. M.; Kroto, H. W. The Detection of HC9N in Interstellar Space. *Astrophys. J.* **1978**, *223*, L105−L107.

(18) Avery, L. W.; Broten, N. W.; MacLeod, J. M.; Oka, T.; Kroto, H. W. Detection of the Heavy Interstellar Molecule Cyanodiacetylene. *Astrophys. J.* **1976**, *205*, L173−L175.

(19) Belloche, A.; Garrod, R. T.; Müller, H. S. P.; Menten, K. M. Detection of a Branched Alkyl Molecule in the Interstellar Medium: Iso-Propyl Cyanide. *Science* **2014**, *345*, 1584−1587.

(20) Turner, B. E. Detection of Interstellar Cyanoacetylene. *Astrophys. J.* **1971**, *163*, L35−L39.

(21) Winnewisser, G.; Walmsley, C. M. The Detection of HC5N and HC7N in IRC+10216. *Astron. Astrophys.* **1978**, *70*, L37−L39.

(22) Biennier, L.; Carles, S.; Cordier, D.; Guillemin, J.-C.; Le Picard, S. D.; Faure, A. Low Temperature Reaction Kinetics of CN^- + HCCCN and Implications for the Growth of Anions in Titan's Atmosphere. *Icarus* **2014**, *227*, 123−131.

(23) Cordiner, M. A.; Nixon, C. A.; Teanby, N. A.; Irwin, P. G. J.; Serigano, J.; Charnley, S. B.; Milam, S. N.; Mumma, M. J.; Lis, D. C.; Villanueva, G. ALMA Measurements of the HNC and HCCCN Distributions in Titan's Atmosphere. *Astrophys. J. Lett.* **2014**, *795*, L30.

(24) Cordiner, M. A.; Palmer, M. Y.; Nixon, C. A.; Irwin, P. G. J.; Teanby, N. A.; Charnley, S. B.; Mumma, M. J.; Kisiel, Z.; Serigano, J.; Kuan, Y.-J. Ethyl Cyanide on Titan: Spectroscopic Detection and Mapping Using ALMA. 2014, *arXiv:1410.5325*. arXiv.org e-Print archive. http://arxiv.org/abs/1410.5325 (accessed Jan 2015).

(25) Loison, J. C.; Hébrard, E.; Dobrijevic, M.; Hickson, K. M.; Caralp, F.; Hue, V.; Gronoff, G.; Venot, O.; Bénilan, Y. The Neutral

DOI: 10.1021/acs.jpclett.5b00519
J. Phys. Chem. Lett. 2015, 6, 1599−1604

Photochemistry of Nitriles, Amines and Imines in the Atmosphere of Titan. *Icarus* **2015**, *247*, 218−247.
(26) Sims, I. R.; Queffelec, J.-L.; Travers, D.; Rowe, B. R.; Herbert, L. B.; Karthäuser, J.; Smith, I. W. M. Rate Constants for the Reactions of CN with Hydrocarbons at Low and Ultra-Low Temperatures. *Chem. Phys. Lett.* **1993**, *211*, 461−468.
(27) Sims, I. R.; Queffelec, J.-L.; Defrance, A.; Rebrion-Rowe, C.; Travers, D.; Bocherel, P.; Rowe, B. R.; Smith, I. W. M. Ultralow Temperature Kinetics of Neutral−Neutral Reactions. The Technique and Results for the Reactions CN+O_2 down to 13 K and CN+NH_3 down to 25 K. *J. Chem. Phys.* **1994**, *100*, 4229.
(28) Rowe, B. R.; Parent, D. C. Techniques for the Study of Reaction Kinetics at Low Temperatures Application to the Atmospheric Chemistry of Titan. *Planet. Sp. Sci.* **1995**, *43*, 105−l 14.
(29) Cheikh Sid Ely, S.; Morales, S. B.; Guillemin, J.-C.; Klippenstein, S. J.; Sims, I. R. Low Temperature Rate Coefficients for the Reaction CN + HCCCN. *J. Phys. Chem. A* **2013**, *117*, 12155−12164.
(30) Carty, D.; Page, V. Le; Sims, I. R.; Smith, I. W. M. Low Temperature Rate Coe Cients for the Reactions of CN and C2H Radicals with Allene CH_2═C═CH_2 and Methyl Acetylene (CH_3CCH). *Chem. Phys. Lett.* **2001**, *344*, 310−316.
(31) Morales, S. B.; Le Picard, S. D.; Canosa, A.; Sims, I. R. Experimental Measurements of Low Temperature Rate Coefficients for Neutral-Neutral Reactions of Interest for Atmospheric Chemistry of Titan, Pluto, and Triton: Reactions of the CN Radical. *Faraday Discuss. Chem. Soc.* **2010**, *147*, 155−171.
(32) Kaiser, R. I. Experimental Investigation on the Formation of Carbon-Bearing Molecules in the Interstellar Medium via Neutral-Neutral Reactions. *Chem. Rev.* **2002**, *102*, 1309−1358.
(33) Kaiser, R. I.; Balucani, N. The Formation of Nitriles in Hydrocarbon-Rich Atmospheres of Planets and Their Satellites: Laboratory Investigations by the Crossed Molecular Beam Technique. *Acc. Chem. Res.* **2001**, *34*, 699−706.
(34) Balucani, N.; Asvany, O.; Kaiser, R.-I.; Osamura, Y. Formation of Three C4H3N Isomers from the Reaction of CN (X2Σ+) with Allene, H_2CCCH_2 (X1A1), and Methylacetylene, CH_3CCH (X1A1): A Combined Crossed Beam and Ab Initio Study. *J. Phys. Chem. A* **2002**, *106*, 4301−4311.
(35) Balucani, N.; Asvany, O.; Huange, L. C. L.; Lee, Y. T.; Kaiser, R. I.; Osamura, Y.; Bettinger, H. F. Formation of Nitriles in the Interstellar Medium via Reactions of Cyano Radicals, CN (X2S+), with Unsaturated Hydrocarbons. *Astrophys. J.* **2000**, *545*, 892−906.
(36) Abeysekera, C.; Joalland, B.; Shi, Y.; Kamasah, A.; Oldham, J. M.; Suits, A. G. Note: A Short-Pulse High-Intensity Molecular Beam Valve Based on a Piezoelectric Stack Actuator. *Rev. Sci. Instrum.* **2014**, *85*, 116107.
(37) Steber, A. L.; Harris, B. J.; Neill, J. L.; Pate, B. H. An Arbitrary Waveform Generator Based Chirped Pulse Fourier Transform Spectrometer Operating from 260 to 295 GHz. *J. Mol. Spectrosc.* **2012**, *280*, 3−10.
(38) Haipern, J. B.; Jackson, W. M. Partitioning of Excess Energy in the Photolysis of Cyanogen Chloride and Cyanogen Bromlde at 193 Nm. *J. Phys. Chem.* **1982**, *4794*, 3528−3533.
(39) Division, L. C. Photodissociation of C2N2, CICN, and BrCN in a Pulsed Molecular Beam. *J. Phys. Chem.* **1984**, *88*, 3419−3425.
(40) Robinson, J. C.; Sveum, N. E.; Goncher, S. J.; Neumark, D. M. Photofragment Translational Spectroscopy of Allene, Propyne, and Propyne-d3 at 193 Nm. *Mol. Phys.* **2005**, *103*, 1765−1783.
(41) The Cologne Database for Molecular Spectroscopy, CDMS. http://www.astro.uni-koeln.de/cdms (accessed January 2, 2015).
(42) Huang, C. H.; Kaiser, R. I.; Chang, A. H. H. Theoretical Study on the Reaction of Ground State Cyano Radical with Propylene in Titan's Atmosphere. *J. Phys. Chem. A* **2009**, *113*, 12675−12685.

DOI: 10.1021/acs.jpclett.5b00519
J. Phys. Chem. Lett. 2015, 6, 1599−1604